Fast synaptic transmission between striatal spiny projection neurons

Uwe Czubayko*† and Dietmar Plenz*‡

*Unit of Neural Network Physiology, Laboratory of Systems Neuroscience, National Institute of Mental Health, 9000 Rockville Pike, Bethesda, MD 20892; and †Department of Anatomy and Neurobiology, University of Tennessee College of Medicine, 875 Monroe Avenue, Memphis, TN 38163

Edited by Ann M. Graybiel, Massachusetts Institute of Technology, Cambridge, MA, and approved October 2, 2002 (received for review July 18, 2002)

Striatal inhibition plays an important role in models of cortex-basal ganglia function and is altered in many basal ganglia diseases. The γ-aminobutyric acid ergic spiny projection neuron comprises >95% of striatal neurons, but despite strong anatomical evidence, the electrophysiological properties and functions of their local axon collaterals are unknown. We simultaneously recorded from adjacent spiny projection neurons (<5–10 μm) in whole-cell patch mode and demonstrated a fast synaptic connection between 26/69 pairs in cortex-striatum-substantia nigra organotypic cultures and 5/38 pairs in acute striatal slices. The synapse, which was blocked by γ-aminobutyric acid type A antagonists, displayed a wide range of failure rates, was depolarizing at rest, and reversed above −60 mV. Presynaptic bursts of action potentials were highly correlated with total postsynaptic depolarization at rest. Synaptic transmission was optimized for burst discharge >14 Hz and showed considerable short-term plasticity, including paired-pulse depression at intervals <25 ms, intraburst facilitation, and interburst augmentation. This activity-dependent collateral interaction provides the basis for a new class of basal ganglia models in which striatal neurons cooperate as well as compete during processing of cortical inputs.

Information from cortex is processed in several parallel pathways by the basal ganglia and sent back to the cortex via thalamus (1). In these cortex–basal ganglia loops, the striatum is the first stage where inputs from many cortical areas converge onto γ-aminobutyric acid (GABA)ergic spiny projection neurons (2), which comprise >95% of the striatum. Cortical inputs depolarize these neurons from resting potential, the down-state, to a subthreshold membrane potential range, the up-state, during which spiny projection neurons fire episodic bursts of action potentials (3). Because these neurons directly inhibit neurons in globus pallidus and substantia nigra, which constitute basal ganglia outputs, understanding the factors that control up-state generation and action potential firing in spiny projection neurons is a prerequisite for understanding basal ganglia function.

Since their first anatomical description by Ramon y Cajal (4), it has been known that spiny projection neurons, in addition to projecting out of the striatum, possess extensive local axon collaterals (5, 6) and make synaptic contacts among each other (7, 8). This view led in many basal ganglia models to treat the striatum as a lateral inhibition network (9–13) in which cortical inputs compete at the striatal level for control of basal ganglia outputs. Despite this popular view of striatal function, however, direct electrophysiological evidence of synaptic transmission between identified spiny projection neurons has been elusive (14). This discrepancy implied that intrastriatal synaptic inhibition is dominated by few striatal GABAergic interneurons (15), in particular fast spiking interneurons (16, 17). Because an imbalance of striatal GABAergic transmission is at the core of many basal ganglia diseases (18), the role of axon collaterals of spiny projection neurons is of particular importance for understanding basal ganglia function and dysfunction.

The modulation of up-states through local axon collaterals by spiny projection neurons, and thus interaction between cortex-basal ganglia loops, most likely will include lateral cooperation as well as lateral competition in an activity-dependent manner. First, the very negative resting membrane potential (V_{Rest}) of −90 mV (6) and the more depolarized GABA type A ($GABA_A$) chloride reversal potential (E_{Cl}) at −60 mV (19) constitutes an electrophysiological hallmark for mature spiny projection neurons. Thus, fast GABAergic transmission can exert depolarizing as well as hyperpolarizing effects depending on the postsynaptic membrane potential. Second, synapses display facilitation or depression to presynaptic action potential bursts (20). Because spiny projections neurons fire action potential bursts *in vivo* during active movements and sensory inputs (21), understanding short-term plasticity at the synaptic level will be critical for our understanding of local striatal network dynamics.

Methods

Electrophysiology. For the preparation of cortex-striatum–substantia nigra organotypic cultures, coronal brain slices from rat at postnatal days 0–2 that contained cortex, striatum, and substantia nigra were grown for 4–6 wk as described (16). For acute slices, brains from young rats were quickly removed and coronal sections of 300 μm were cut. For electrophysiological recording, cultures or slices were submerged in standard artificial cerebrospinal fluid (ACSF; 300 ± 5 mOsm) containing 126 mM NaCl, 0.3 mM NaH_2PO_4, 2.5 mM KCl, 0.3 mM KH_2PO_4, 1.6 mM $CaCl_2$, 1.0 mM $MgCl_2$, 0.4 mM $MgSO_4$, 26.2 mM $NaHCO_3$, and 11 mM D-glucose saturated with 95% O_2 and 5% CO_2. For acute slice experiments, extracelluar $[K^+]$ was increased to 5 mM to increase V_{Rest} in striatal neurons. Recordings in culture and acute slices were done at 35 ± 0.5°C and room temperature, respectively. Somatic whole-cell patch recordings were obtained by using borosilicate electrodes (4–6 MΩ) containing 132 mM K-gluconate, 6 mM KCl, 8 mM NaCl, 10 mM Hepes, 2 mM Mg-ATP, 0.39 mM Na-GTP, and 0.2% Neurobiotin with pH adjusted to 7.2–7.4 and a final osmolarity of 290 ± 10 mOsm. Tight seals (>2–4 GΩ) were made to somata of visually identified cells and, after breakthrough, intracellular membrane potentials were recorded in current clamp at 25 kHz (Axopatch 200D, Axon Instruments, Foster City, CA), preamplified (Cyberamp380, Axon Instruments), and digitized for further processing in continuous stream mode by using the CED μ1401 (Cambridge Electronic Design, Cambridge, U.K.). For anatomical reconstruction, cultures were fixed in 4% paraformaldehyde overnight and neurons were processed with the ABC Vectastain kit followed by standard diaminobenzidine procedures (all from Vector Laboratories).

Data Analysis. To block the occurrence of spontaneous up-states and fast glutamatergic transmission in culture, all recordings were performed in the presence of the glutamate antagonist 6,7-dinitroquinoxaline-2,3-dione (DNQX, 10 μM). To analyze

This paper was submitted directly (Track II) to the PNAS office.

Abbreviations: GABA, γ-aminobutyric acid; V_{Rest}, resting membrane potential; PSP, postsynaptic potential.

‡To whom correspondence should be addressed. E-mail: plenzd@intra.nimh.nih.gov.

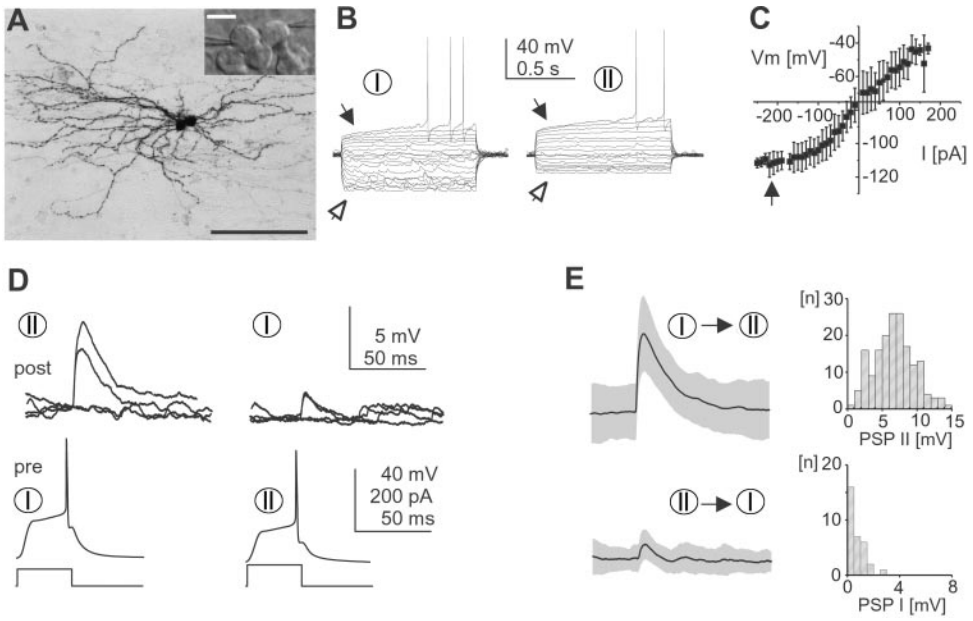

Fig. 1. Cultured striatal spiny projection neurons are connected through a monosynaptic, fast synaptic transmission. (*A*) Anatomical reconstruction of two monosynaptically connected spiny projection neurons from cortex-striatum-substantia nigra organotypic culture (Neurobiotin). (*Inset*) Striatal area during dual whole-cell patch recording from contiguous medium-sized, spherical cell bodies (light-microscopic picture, Hoffman modulation contrast). [Bar = 100 μm, 10 μm in *Inset*.] (*B*) Cultured spiny projection neurons with early rectification on depolarization (filled arrow), delayed action potential firing, and anomalous rectification (open arrow) in response to equidistant somatic current pulses ($V_{Rest\ I} = -81$ mV and $V_{Rest\ II} = -76$ mV). (*C*) I–V relationship for cultured neurons (±SD; $n = 70$). Note the strong anomalous rectification below −100 mV (filled arrow). (*D*) Postsynaptic responses in two reciprocally connected spiny projection neurons from *B* at rest. Four individual responses including two failures are plotted for each connection. Connections had failure rates of 9% (I → II) and 87% (II → I). (*E*) Average PSP and corresponding distribution of peak amplitudes for each connection in *D* (gray area indicates SEM, failures excluded). Same scale as in *D*.

synaptic connections, single action potentials or action potential bursts were evoked by current injection. Postsynaptic potentials (PSPs) were averaged for each direction at resting potential. Each neuron was compared once. Up to 200 responses were averaged for the analysis of synaptic responses to single action potentials. Peak amplitudes were taken from responses 2–20 ms after a presynaptic action potential. Maximal slope value was calculated from a linear approximation of the PSP trajectory between 20% and 80% of maximal amplitudes. Synaptic delay was defined by the midpoint of this slope. Failures were classified as individual responses that did not cross threshold (±3 SD of prestimulus noise) during peak time of the average response (±2 ms). Failure sweeps were excluded for calculation of average PSP values. Postsynaptic responses to bursts of action potentials were integrated after subtracting average prestimulus membrane potentials. Decay time constants of the postsynaptic response after burst termination were fitted with single exponentials normalized to the decay time constant from single PSPs.

Data are expressed as mean ± SEM, if not stated otherwise. For multiple comparisons between classes, an ANOVA with post hoc Scheffé test was used. Correlation was estimated by regression analysis. DNQX (Research Biochemicals), bicuculline-methiodide, and picrotoxin (all Sigma) were bath applied at final concentrations.

Results

Fast GABAergic Synaptic Transmission Between Striatal Spiny Projection Neurons. We recorded simultaneously from striatal spiny projection neurons with contiguous or nearby somata (<5 μm) in organotypic cortex striatum–substantia nigra cultures (16) by using dual whole-cell patch recordings in current clamp (Fig. 1). In these cultures, striatal spiny projection neurons mature properly and show up- and down-state transitions (22), their typical firing pattern *in vivo* as a result of cortical inputs (3). Because dopaminergic inputs from substantia nigra critically regulate striatal electrophysiology (23), the culture system also included the substantia nigra with an anatomically and functionally intact nigrostriatal pathway (24–26).

Spiny projection neurons grown for 36 ± 0.5 d *in vitro* were identified by a small spherical cell body, relatively negative V_{Rest}, anomalous rectification, and long delay to first action potential on current pulse injection (Fig. 1 *A–C* and Table 1). In response to single presynaptic action potentials, 26/69 pairs of cultured neurons revealed a PSP, of which 8/26 pairs were connected reciprocally (Figs. 1 *D* and *E* and 2 *A* and *D*). The PSP was delayed by 3.9 ± 0.2 ms, peaked 8 ± 0.4 ms after spike onset, and had an average amplitude of 2.15 ± 0.38 mV at V_{Rest} (Fig. 2 *B* and *C*). Correlation between maximal slope and amplitude peak was $r = 0.79$ ($P < 0.0001$). In reciprocally connected pairs, one connection dominated at PSP amplitudes >3 mV (Fig. 2*D*). Average PSP amplitude was independent of V_{Rest} (Fig. 2*E*). Synapses with peak amplitudes <3 mV revealed a wide range of failure rates in response to single spikes (Fig. 2*F*). No electrical synapses were found. Anatomically reconstructed cells showed

Table 1. Summary of electrophysiological parameters for striatal spiny projection neurons

	Culture	Slice
Neurons, *N*	73	89
Age, days	36 ± 0.5	11 ± 0.5
V_{Rest}, mV	−75 ± 1	−67 ± 1
Input resistance, MΩ	531 ± 4	642 ± 4
Time constant, ms	15.4 ± 0.9	29.7 ± 1.6
Spike width, ms	1.64 ± 0.05	2 ± 0.04
Spike amplitude, mV*	66 ± 0.8	75 ± 0.8
Temperature, °C	35 ± 0.5	≈23

*Measured from threshold to peak.

NEUROSCIENCE

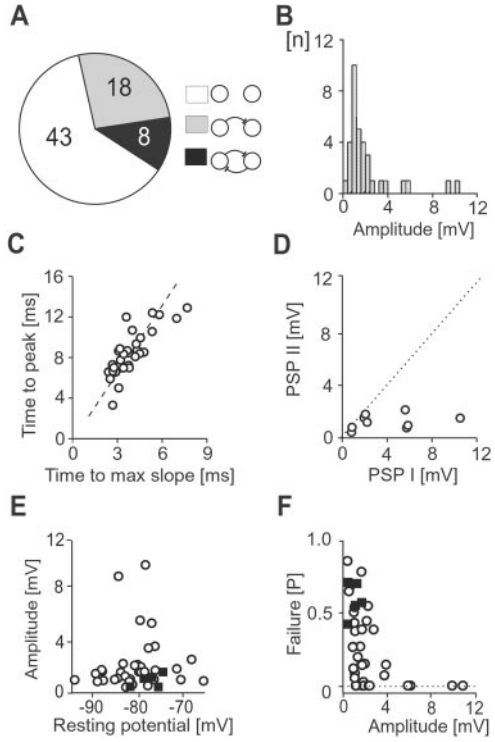

Fig. 2. Synaptic transmission between spiny projection neurons is depolarizing at rest and characterized by a wide range of failure rates. (*A*) Summary of unconnected and asymmetrically or reciprocally connected paired recordings (numbers) in culture. (*B*) Distribution of average peak amplitudes. (*C*) Scatter plot of time to maximal slope time and peak amplitude. Broken line indicates linear regression. (*D*) Scatter plot for PSP amplitudes of reciprocally connected pairs. Dotted line indicates identical PSP values. (*E* and *F*) Scatter plots of resting potential vs. peak amplitude and synaptic failure rates vs. average peak amplitude. ○, Culture; ■, acute slice.

typical characteristics of spiny projection neurons including a spherical cell body, spiny higher order dendrites, and extensive local axon collaterals (Fig. 1*A*, $n = 6$).

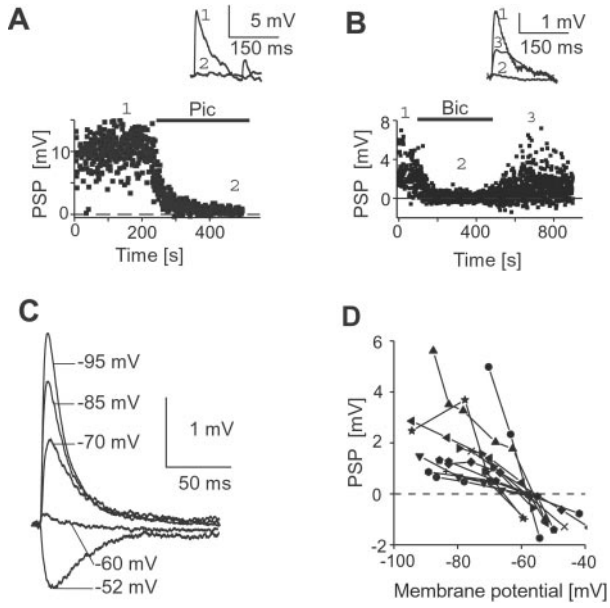

Fig. 4. The GABAergic monosynaptic transmission between spiny projection neurons reverses at −60 mV. (*A* and *B*) The PSP is blocked by bath application of picrotoxin (pic, 50 μM) or bicuculline (bic, 20 μM). (*Insets*) Traces from periods indicated by numbers. (*C*) Reversal of PSP as a function of membrane potential. Traces are aligned at average membrane potential before stimulation (averages are from 30–50 responses each). Note prolonged decay at depolarized potentials because of closure of anomalous rectifier. (*D*) Summary of the reversal in GABAergic synaptic responses ($n = 11$ neurons, all culture). Peak PSP response plotted against average membrane potential shifted by steady-state current injection before stimulus.

The existence of this monosynaptic connection was further demonstrated in young, acute striatal slices (postnatal day 11 ± 0.5). Spiny projection neurons were identified by a small spherical cell body, anomalous rectification, and long delay to first action potential on current pulse injections (Fig. 3 *A–C* and Table 1) All neuronal pairs were recorded at 50–100 μm from the slice surface, and their somata were separated by <10 μm.

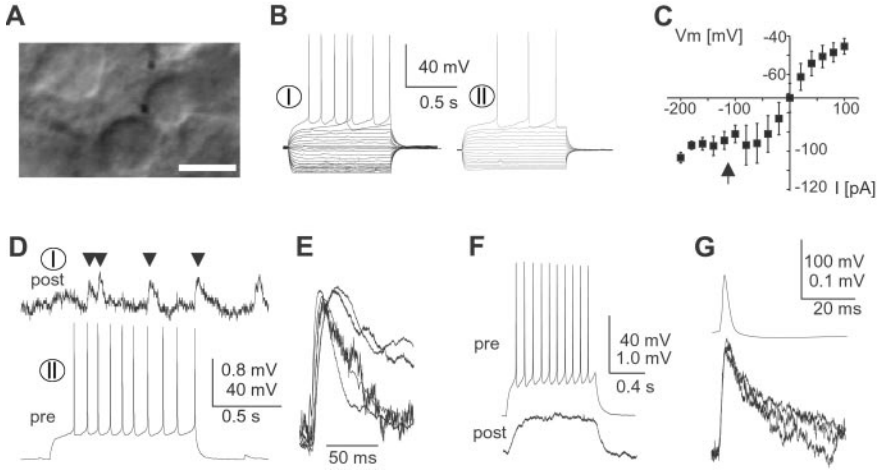

Fig. 3. Spiny projection neurons in acute striatal slices are connected through a monosynaptic, fast synaptic connection. (*A*) Acute striatal slice with contiguous medium-sized, spherical cell bodies during dual whole-cell patch recording. (Bar = 10 μm.) (*B*) Responses of spiny projection neurons to current injections ($V_{Rest\ I} = -62$ mV and $V_{Rest\ II} = -68$ mV). (*C*) I–V relationship for spiny projection neurons from acute slices ($n = 89$). Note the strong anomalous rectification below −90 mV (filled arrow). (*D*) Synaptic connection between spiny projection neurons in acute striatal slices (same neurons as in *B*). Note the high failure rate. (*E*) Overplot of average responses (failures excluded) for all five connected pairs normalized by amplitude. (*F*) Electrical synapse in a pair of spiny projection neurons (acute slice; $V_{Rest\ pre} = -62$ mV and $V_{Rest\ post} = -74$ mV). (*G*) Typical spikelet in electrically coupled spiny projection neurons at three different membrane potentials (−70, −60, and −50 mV). pre, presynaptic; post, postsynaptic.

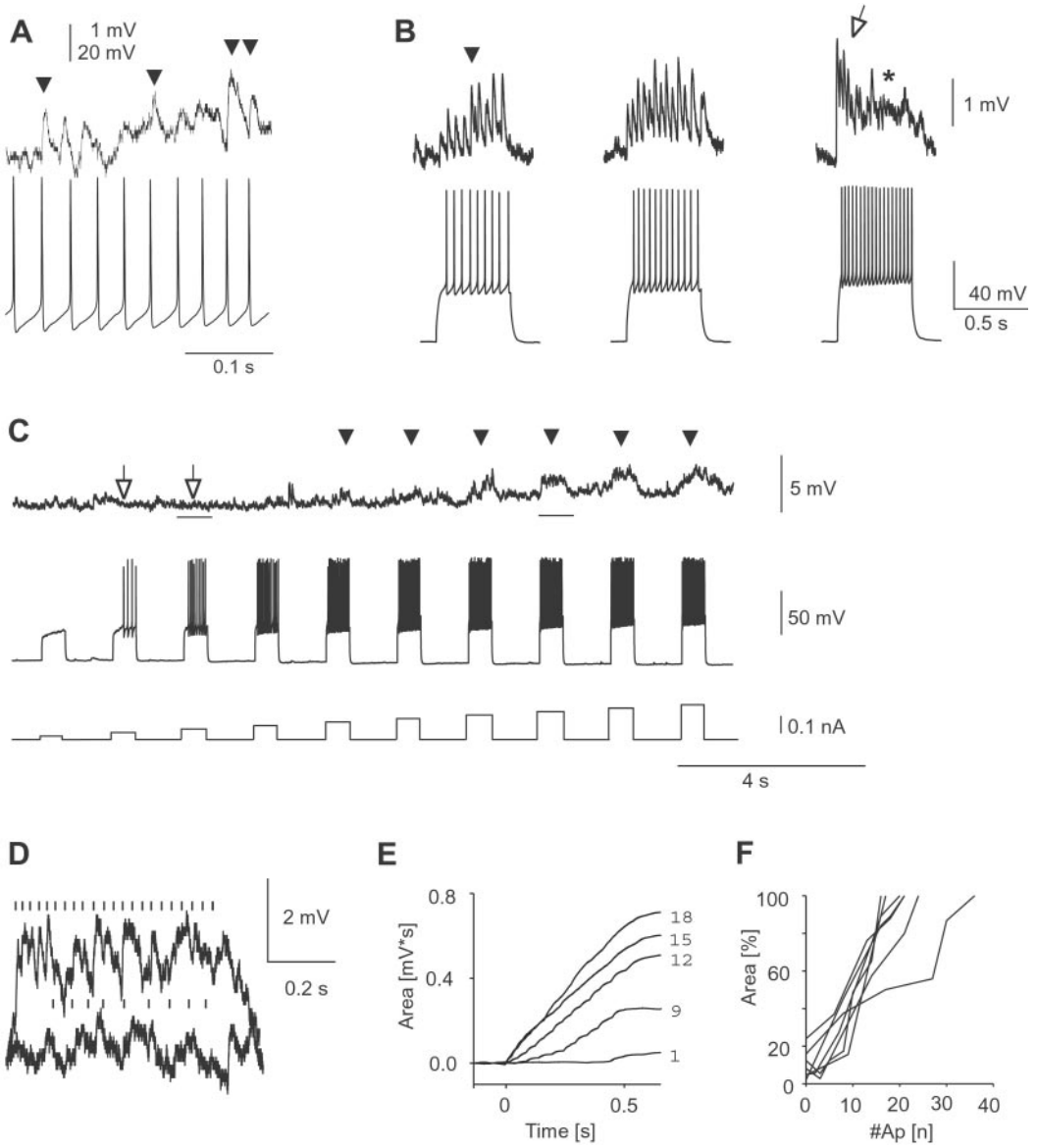

Fig. 5. Postsynaptic depolarization in spiny projection neurons is linearly correlated with number of presynaptic action potentials during burst firing. (*A*) Connection with high failure rate at 35 Hz presynaptic burst firing ($V_{Rest\ post} = -74$ mV). (*B*) Change in PSP amplitudes during presynaptic action potential bursts at different burst frequencies. (*Left*) Increasing PSP amplitudes at 18 Hz (filled arrow). (*Center*) Relatively constant PSP amplitudes at 24 Hz. (*Right*) Facilitated PSP responses during early burst period (open arrow) followed by decreased PSP amplitudes that merge into a plateau-like depolarization at 36 Hz (*). Same neuron ($V_{Rest\ pre} = -80$ mV and $V_{Rest\ post} = -83$ mV). (*C*) Uncovering of synaptic steady-state depolarization during high frequency bursts (arrowheads). PSP in response to presynaptic bursts of action potentials at increasing burst frequency. Note absence of postsynaptic response at low burst frequency (open arrows; $V_{Rest\ pre} = -68$ mV and $V_{Rest\ post} = -87$ mV). Note also slow depolarization that recovers 35 s after burst series. (*D*) Overlay plot of two PSP in response to presynaptic bursts from *C* (time periods indicated by bars). (*E*) Monotone increase of integrated PSP area over time during 500-ms lasting presynaptic bursts (numbers of action potentials indicated on the right). (*F*) Total postsynaptic depolarization is linearly correlated with number of presynaptic action potentials (500-ms current pulse duration; $n = 8$ neurons, all culture).

In 5 of 38 pairs a synaptic connection was found (Fig. 3 *D* and *E*). Responses to single action potentials and bursts of action potentials revealed failure rates ≈0.5 (Figs. 2*F* and 3*D*). PSP amplitudes were not significantly different between culture and acute slice (Fig. 2*E*, $P > 0.08$). Four additional pairs (4 of 38) were coupled electrically (27), which was mostly revealed by spikelets using spike triggered averaging. The amplitude ratio was 0.28 ± 0.07% for spikes (Fig. 3 *F* and *G*). No differences in electrophysiological parameters were found between connected and nonconnected pairs for culture or acute slice preparation.

Bath application of the $GABA_A$-channel blocker picrotoxin or $GABA_A$-receptor antagonist bicuculline (Fig. 4 *A* and *B*) significantly reduced the postsynaptic response by 93 ± 1.4% (50 μM; $n = 3$, $P < 0.001$) and by 95.2 ± 3.4%, respectively (20 μM, $n = 2$; $P < 0.001$, two-tailed *t* test). After washout of bicuculline, the response recovered to 84.2 ± 7.3% of control. By varying the average membrane potential through steady-state current injection, PSPs were found to reverse in polarity at −60 ± 2 mV ($n = 11$), which is near the expected chloride reversal potential $E_{Cl} = -59$ mV in our preparation (Fig. 4 *C* and *D*).

Synaptic Transmission Between Striatal Spiny Projection Neurons Is Optimized for Action Potential Bursts and Carries a Short-Term Memory of at Least 1 s. Depending on their release probabilities, synapses can display considerable depression or facilitation in

response to presynaptic bursts of action potentials (20). This short-term plasticity has important implications for network functions (e.g., ref. 28). Given the wide range in synaptic failure rates, i.e., release probabilities for synaptic transmission between spiny projection neurons (Fig. 2*F*), it is therefore important to understand the dynamics of these synapses to brief episodes of action potential bursts, the typical firing mode of striatal projection neurons *in vivo* during active movements and sensory inputs (21). Although high failure rates persisted in some neurons even at high presynaptic burst frequencies (Fig. 5*A*), in many neurons the integrated PSP response was monotonically increasing over time during a burst, resulting in profound postsynaptic depolarization at high burst frequencies (Fig. 5*B*). For some monosynaptic connections, postsynaptic depolarizations were only revealed during high presynaptic burst frequencies (Fig. 5 *C* and *D*). No significant depression was found and integrated postsynaptic depolarization was tightly correlated with action potential number per burst (Fig. 5 *E* and *F*; $r = 0.97 \pm 0.001$, $n = 8$ neurons). Thus, presynaptic burst strength directly translates into postsynaptic depolarization at rest.

Furthermore, synaptic interaction between spiny projection neurons was optimized for burst activity above a critical threshold. First, paired-pulse depression of PSPs was present at interspike intervals <25 ms (Fig. 6*A*; $n = 8$ neurons, $P < 0.05$) reducing the postsynaptic effect of short bursts. Second, many synapses facilitated during prolonged bursts at low frequency (Fig. 5*B*). Third, after prolonged bursts above 16 Hz, postsynaptic responses were characterized by a plateau-like depolarization with less distinct individual PSPs that outlasted presynaptic bursts considerably before returning to resting value (Figs. 5*B* and 6 *B* and *C*; $n = 6$ neurons, $P < 0.05$).

Finally, the synaptic connection maintained a memory of at least 1 s with respect to previous burst activity. PSPs to spikes that followed presynaptic bursts after 1 s were increased by up to 100% for burst frequencies above 14 Hz (Figs. 5*B* and 6 *D* and *E*; $n = 9$ neurons, $P < 0.05$). Thus, lateral GABAergic transmission between spiny projection neurons is optimized for burst activity and augments during repetitive burst periods.

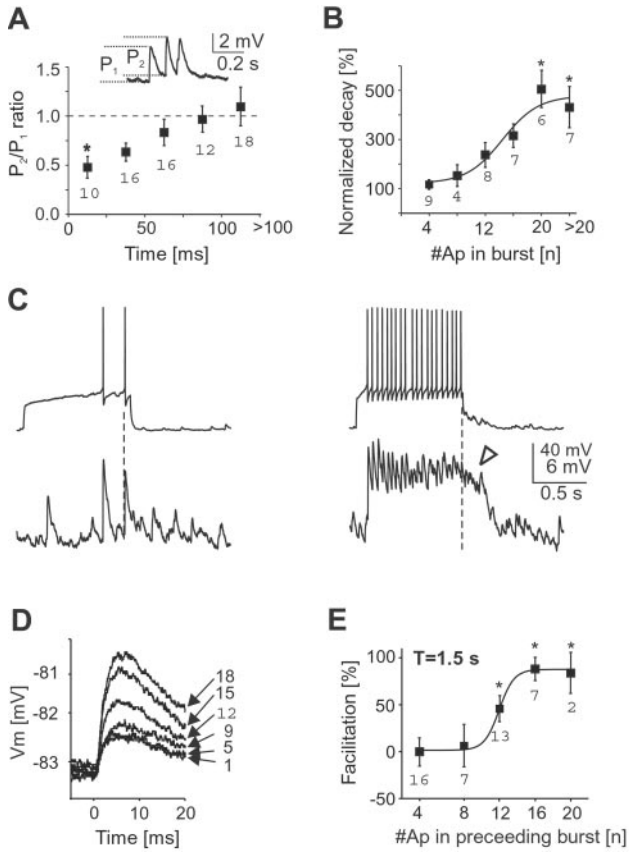

Fig. 6. The postsynaptic depolarization as a result of presynaptic burst activity is increased and prolonged during repetitive bursts. (*A*) Short-term depression of PSP amplitudes between spiny projection neurons. Data taken from first two spikes in bursts below facilitation threshold (*, $P < 0.05$ compared to last two groups, all culture). (*B*) Summary data showing a significantly prolonged decay in postsynaptic depolarization after burst termination at frequencies above 16 Hz (1-s current pulse duration; *, $P < 0.05$ compared to first group, $n = 6$ neurons, all culture). (*C*) Example of prolonged postsynaptic decay after high frequency bursts of 1-s duration (same neuron, open arrow; $V_{Rest\ pre} = -80$ mV and $V_{Rest\ post} = -72$ mV). (*D*) Short-term facilitation of PSP amplitudes by preceding bursts. Overplot of PSP response to the first spike in a burst as a function of number of spikes (right) in the preceding burst (1.5-s interburst interval, same neuron as in Fig. 5*B*). (*E*) If the preceding burst contains more than eight spikes per 500 ms pulse duration (>16 Hz), a single PSP after 1 s is facilitated by up to 100% (*, $P < 0.05$ compared to first group, $n = 9$ neurons, all culture). Numbers in graphs indicate number of cases for each class.

Discussion

We have identified a fast GABAergic connection optimized for burst transmission between striatal spiny projection neurons that substantially depolarizes neurons at rest and reverses at −60 mV. Dual recordings from neurons at distances <10 μm, the use of patch electrodes, and a culture preparation in which local connectivity is preserved probably enhanced the likelihood of finding connected pairs. Despite extensive local axon collaterals, the probability of connected pairs in culture was only ≈30%. Furthermore, reciprocal connections were relatively few and functionally asymmetrical, i.e., one connection dominated. These findings suggests that lateral connections between spiny projection neurons are relatively sparse and mostly asymmetrical within the local neighborhood.

GABAergic synaptic responses described in the current study between identified spiny projection neurons in mature culture are similar to pharmacologically isolated GABAergic responses in mature striatal slices: First, the amplitude of single synaptic GABAergic PSPs shown here is in the range of single synaptic PSPs reported under minimal stimulation conditions (29). Second, synaptic augmentation (30) and paired-pulse depression (29, 30) have also been described for GABAergic responses to extracellular shock stimulation in striatal projection neurons. Furthermore, prolonged PSP decay at high-burst frequencies and plateau-like depolarization during such bursts are reminiscent of asynchronous GABA release that was also described in dual recordings from unidentified striatal neurons in dissociated cultures (31).

From the present study, three main aspects arise for intrastriatal GABAergic synaptic transmission. First, the GABAergic transmission between spiny projection neurons is sufficient to induce a steady-state depolarization in postsynaptic neurons. The reversal potential of chloride in spiny projection neurons *in vivo* is at −60 mV (19), which is up to 30 mV above their resting potential (6). Compartmental model studies suggest such depolarization to be sufficient to reduce the anomalous rectifier at rest, which would facilitate further depolarization from cortical inputs in the postsynaptic neuron (32). Because GABAergic synapses are made along the dendritic tree (2), the reduction in electrotonic length from closure of the anomalous rectifier would "uncover" synaptic connections at high presynaptic burst frequencies as was found in our experiments (see Fig. 5 *C* and *D*). Such local GABAergic transmission will play an important role in the facilitation and/or modulation of transitions to up-states (3) thereby changing a neuron's response to cortical inputs (11). Furthermore, depolarizing GABAergic synapses

have been shown to play an important role in synaptic plasticity during development (33) and could underlie the development of "matrisomes" in the corticostriatal pathway (34, 35). These cooperative effects are in contrast to the competitive effect, when the postsynaptic neuron's membrane potential is at or above −60 mV. At these depolarized levels, fast inhibitory transmission allows spiny projection neurons to shunt and/or hyperpolarize each other and thereby to precisely control temporal firing of action potentials (30). Both cooperative and competitive effects will be optimal for action potential bursts frequencies above 14 Hz.

The demonstration of a fast, GABAergic synaptic connection between striatal projection neurons allows the general class of lateral inhibition networks to be applied to striatal function. Lateral inhibition between striatal projection neurons has been suggested to govern voluntary movements (9), has been implemented in models about prefrontal cognitive aspects of serial order in behavior (12), is crucial in models of reinforcement learning as a function of dopamine (13), has been proposed to be increased under reduced levels of dopamine, thereby inducing a parkinsonian state of motor arrest (10), and has been suggested to allow striatal neurons to code for temporal sequences of cortical activity (11). Our results, while providing experimental evidence for these models on cortex-basal ganglia function, extend these views, and demonstrate that lateral synaptic transmission between spiny projection neurons is asymmetrical, highly dynamic, and serves cooperative as well as competitive functions.

Note. While this paper was in revision, Tunstall *et al.* (36) reported a fast GABAergic response to single action potentials between spiny projection neurons by using dual sharp intracellular recordings in acute striatal slices.

We thank V. Karpiak and C. V. Stewart for expert technical assistance, and Drs. J. Beggs, C. Gerfen, J. Kerr, and C. McBain for comments on an early draft of the manuscript. This work was supported by the National Institute of Mental Health and the National Institute of Neurological Disorders and Stroke (NS-26473-11).

1. Alexander, G. E., Crutcher, M. D. & DeLong, M. R. (1990) *Prog. Brain Res.* **85,** 119–146.
2. Smith, A. D. & Bolam, J. P. (1990) *Trends Neurosci.* **13,** 259–265.
3. Wilson, C. J. & Kawaguchi, Y. (1996) *J. Neurosci.* **16,** 2397–2410.
4. Ramon y Cajal, S. (1911) *Histologie du Systeme Nerveux de l'Homme et des Vertebres* (Maloine, Paris); trans. Swanson, N. & Swanson, L. W. (1995) *Histology of the Nervous System* (Oxford Univ. Press, London), Vol. 2.
5. Preston, R. J., Bishop, G. A. & Kitai, S. T. (1980) *Brain Res.* **183,** 253–263.
6. Kawaguchi, Y., Wilson, C. J. & Emson, P. C. (1989) *J. Neurophysiol.* **62,** 1052–1068.
7. Somogyi, P., Bolam, J. P. & Smith, A. D. (1981) *J. Comp. Neurol.* **195,** 567–584.
8. Yung, K. K., Smith, A. D., Levey, A. I. & Bolam, J. P. (1996) *Eur. J. Neurosci.* **8,** 861–869.
9. Groves, P. M. (1983) *Brain Res.* **5,** 109–132.
10. Wickens, J. R., Kötter, R. & Alexander, M. E. (1995) *Synapse* **20,** 281–298.
11. Plenz, D., Wickens, J. R. & Kitai, S. T. (1996) in *Computational Neuroscience*, ed. Bower, J. M. (Academic, San Diego), pp. 397–402.
12. Beiser, D. G. & Houk, J. C. (1998) *J. Neurophysiol.* **79,** 3168–3188.
13. Suri, R. E. & Schultz, W. (1998) *Exp. Brain Res.* **121,** 350–354.
14. Jaeger, D., Kita, H. & Wilson, C. J. (1994) *J. Neurophysiol.* **72,** 2555–2558.
15. Kawaguchi, Y., Wilson, C. J., Augood, S. J. & Emson, P. C. (1995) *Trends Neurosci.* **18,** 527–535.
16. Plenz, D. & Kitai, S. T. (1998) *J. Neurosci.* **18,** 266–283.
17. Koos, T. & Tepper, J. M. (1999) *Nat. Neurosci.* **2,** 467–472.
18. Albin, R. L., Young, A. B. & Penney, J. B. (1989) *Trends Neurosci.* **12,** 366–375.
19. Mercuri, N. B., Calabresi, P., Stefani, A., Stratta, F. & Bernardi, G. (1991) *Synapse* **8,** 38–40.
20. Thomson, A. M. (2000) *Trends Neurosci.* **23,** 305–312.
21. DeLong, M. R. (1973) *Science* **179,** 1240–1242.
22. Plenz, D. & Aertsen, A. (1996) *Neuroscience* **70,** 893–924.
23. Nicola, S. M., Surmeier, J. & Malenka, R. C. (2000) *Annu. Rev. Neurosci.* **23,** 185–215.
24. Plenz, D. & Kitai, S. T. (1996) *Neurosci. Lett.* **209,** 177–180.
25. Plenz, D. & Kitai, S. T. (1998) *J. Neurosci.* **18,** 4133–4144.
26. Becq, H., Bosler, O., Geffard, M., Enjalbert, A. & Herman, J. P. (1999) *J. Neurosci. Res.* **58,** 553–566.
27. O'Donnell, P. & Grace, A. A. (1997) *Neuroscience* **76,** 1–5.
28. Abbott, L. F., Varela, J. A., Sen, K. & Nelson, S. B. (1997) *Science* **275,** 220–224.
29. Radnikow, G., Rohrbacher, J. & Misgeld, U. (1997) *J. Neurophysiol.* **77,** 427–434.
30. Fitzpatrick, J. S., Akopian, G. & Walsh, J. P. (2001) *J. Neurophysiol.* **85,** 2088–2099.
31. Behrends, J. C. & Ten Bruggencate, G. (1998) *J. Neurophysiol.* **79,** 2999–3011.
32. Wilson, C. J. (1992) in *Single Neuron Computation*, eds. McKenna, T., Davis, J. & Zornetzer, S. F. (Academic, San Diego), pp. 141–171.
33. Ben Ari, Y., Khazipov, R., Leinekugel, X., Caillard, O. & Gaiarsa, J. L. (1997) *Trends Neurosci.* **20,** 523–529.
34. Malach, R. & Graybiel, A. M. (1986) *J. Neurosci.* **6,** 3436–3458.
35. Parthasarathy, H. B., Schall, J. D. & Graybiel, A. M. (1992) *J. Neurosci.* **12,** 4468–4488.
36. Tunstall, M. J., Oorschot, D. E., Kean, A. & Wickens, J. R. (2002) *J. Neurophysiol.* **88,** 1263–1269.